

Probing Flat Band of Optically-Trapped Spin-Orbital Coupled Bose Gases Using Bragg Spectroscopy

Wu Li¹, Lei Chen¹, Zhu Chen², Ying Hu³, Zhidong Zhang¹, and Zhaoxin Liang^{1*}

¹ *Shenyang National Laboratory for Materials Science,*

Institute of Metal Research, CAS, Wenhua Road, 72, Shenyang, China

² *National Key Laboratory of Science and Technology on Computational Physics,*

Institute of Applied Physics and Computational Mathematics, Beijing 100088, China and

³ *Institute for Quantum Optics and Quantum Information of the Austrian Academy of Sciences, A-6020 Innsbruck, Austria*

Motivated by the recent efforts in creating the flat band in ultracold atomic systems, we investigate how to probe the flat band in an optically-trapped spin-orbital coupled Bose-Einstein condensate using Bragg spectroscopy. We have found that the excitation spectrum and the dynamic structure factor of the condensate alter dramatically, when the band structure exhibits various level of flatness. In particular, when the band exhibits perfect flatness around the band minima corresponding to a near infinite effective mass, a quadratic dispersion emerges in the low-energy excitation spectrum; in sharp contrast, for the opposite case when an ordinary band is present, the familiar linear dispersion arises. Such linear-to-quadratic crossover in the energy spectrum presents a striking manifestation of the transition of an ordinary band into a flat band, thereby allows the direct probe of the flat band by using Bragg spectroscopy.

PACS numbers: 03.75.Kk, 67.85.-d, 64.70.Rh

At present, there have been intensive efforts in realising flat bands in various context of condensed-matter [1] and atomic physics [2–6]. The motivation behind this search is twofold. First, a flat band, whose kinetic energy is highly quenched compared to the scale of interactions, possesses macroscopic level degeneracy, and as a result, interactions play a dominant role in affecting the system which has given rise to many interesting quantum phases [3]. Second, even more challenging is to create topological flat bands with nonzero Chern number [7], which can open a new avenue for engineering fractional topological quantum insulator [1, 2] without Landau levels prompted by the analogy to Landau levels [8] in condensed matter physics. Recently, several proposals on realising flat bands using ultra-cold systems have been reported [2–7, 9]. Along this direction, an important question that naturally arises consists in how to probe the flatness of the created band in these systems.

In this work, we explore the possibility of using Bragg spectroscopy to probe an arising isolated flat band in an optically-trapped spin-orbital-coupled (SOC) Bose-Einstein condensate (BEC). The key ingredient of our approach consists in investigating how the excitation spectrum and dynamic structure factor of the system change when the band structure varies its flatness. Our main results are: (1) a quadratic dispersion $\epsilon(k) \sim k^2$ emerges in the low-energy excitation spectrum, if the band is perfectly flat in the vicinity of energy band minima (corresponding to an infinite effective mass); contrasting sharply, in the opposite case when the BEC has an ordinary band, the familiar linear dispersion relation $\epsilon(k) \sim k$ is found; (2) the static structure factor $S(k)$

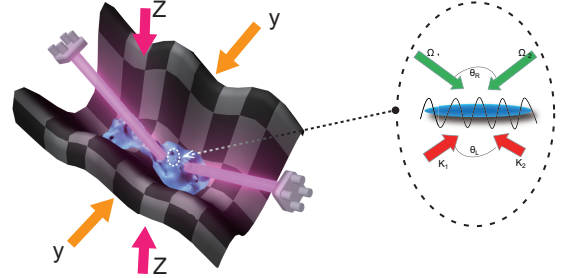


FIG. 1. (color online). Left panel: Bragg spectroscopy probes a single-particle flat band generated by an optically-trapped SO coupled Bose gas. Right panel: schematic setup for implementing a flat band realized in 1D SO-coupled Bose gas proposed by Ref. [9]. Here, Ω_1 and Ω_2 are the Rabi frequencies of the Raman lasers for generating SO coupling. The other two laser beams labeled by \mathbf{k}_1 and \mathbf{k}_2 generate an optical lattice. Bragg spectroscopy can be theoretically described by the dynamic structure factor of the model system.

exhibits a crossover from linear ($S(k) \sim k$) to quadratic relation ($S(k) \sim k^2$) in the momenta, when the band transforms from the ordinary into the flat band. Moreover, by relating the flatness of band with the effective mass at the band minima, and by using Feynmann's relation $\epsilon(k) = \epsilon_0(k)/S(k)$ [10–12], we are able to directly connect the emerging quadratic dispersion in a perfect flat band case with the vanishingly small kinetic energy in the single-particle energy $\epsilon_0(k)$, and thereby establishing Bragg Spectroscopy as an efficient tool to probe the flat band in an optically-trapped SOC BEC.

The setting we consider to probe a flat band in a quasi-1D optically trapped BEC with SOC is illustrated in Fig. 1. Experimentally, it can be realized by combining the Bragg spectroscopy [13, 14] and SOC [15–17] that are

* E-mail: zhxliang@imr.ac.cn

available in both BECs [18] and degenerated fermi gases [19]. In particular, Bragg spectroscopy has become a routine for investigating the excitation spectrum in ultracold atomic systems. Theoretically, the Gross-Pitaevskii equation (GPE) has been shown to well describe, at the mean-field level, both the static and the dynamic properties of a BEC with SOC [9, 20–23]. The validity of the GPE can be tested a posteriori by evaluating the quantum depletion of the condensate. In what follows, we shall begin with briefly describing the model system in which a flat band can arise following Ref. [9], and then show how Bragg spectroscopy can present as an efficient tool to quantitatively probe the presence of a flat band.

Emerging flat bands in a SO coupled BEC.— The considered system is illustrated in Fig. 1, which consists of a BEC with SOC that is trapped in a strongly anisotropic lattice potential. The transverse lattice confinement is sufficiently strong to freeze the atomic motion in these directions, allowing the atomic tunneling only in the x -direction. This realizes an optically trapped quasi-1D BEC with SOC, which can be well described by the celebrated GPE [9, 20–23],

$$i\hbar \frac{\partial \Psi}{\partial t} = (H_0 + H_{\text{int}}) \Psi, \quad (1)$$

with $\Psi = (\psi_{\uparrow}, \psi_{\downarrow})^T$ being the two-component condensate wave functions. Hamiltonian H_0 describes non-interacting bosons in a 1D optical lattice with SOC, reading

$$H_0 = \frac{p_x^2}{2m} + \gamma p_x \sigma_z + \Omega \sigma_x + V_0 \times E_R \sin^2(k_L x), \quad (2)$$

where m is the bare atom mass, σ_x and σ_z are the x - and z -component of Pauli matrices, Ω is the Rabi frequency for generating SOC, $\gamma = 2\pi\hbar \sin(\theta_R/2)/(\lambda_R m)$ with λ_R being the wavelength of the two Raman lasers, respectively, and θ_R being the angle between the lasers; V_0 labels the lattice strength in the unit of the recoil energy $E_R = \hbar^2 k_L^2/2m$ with k_L being the wave vector of the lasers creating the optical lattice. Hamiltonian H_{int} describes the hard-core interaction between bosonic atoms, which can be generally written as

$$H_{\text{int}} = \int dx (g_{11} n_{\uparrow}^2 + g_{22} n_{\downarrow}^2 + 2g_{12} n_{\uparrow} n_{\downarrow}), \quad (3)$$

where $n_{\uparrow} = |\psi_{\uparrow}|^2$ and $n_{\downarrow} = |\psi_{\downarrow}|^2$ are the two-component condensate densities, and $g_{ij} = 4\pi\hbar^2 a_{ij}/m$ ($i, j=1$ or 2) is the coupling constant, with a_{ij} being the s -wave scattering length. In this work, we shall limit ourselves to the case when $g_{11} = g_{22} = g_{12} = g = 4\pi\hbar^2 a/m > 0$; in this regime, the striped phase will not appear in the ground state. For later convenience, we rescale GP Eq. (1) into the dimensionless form by introducing $x \rightarrow k_L x$, $t \rightarrow (2E_R/\hbar)t$, $\gamma \rightarrow \gamma/(\hbar k_L/m)$, $\Omega \rightarrow \Omega/2E_R$, and the dimensionless interaction coefficient $c = \sqrt{\omega_y \omega_z} k_L a N/E_R$ with N being the atom number in one unit cell, and ω_y

and ω_z the trapping frequencies in the transverse directions.

The physics of an optically-trapped quasi-1D BEC with SOC is governed by the interplay among four parameters: the SOC parameters γ and Ω , lattice strength V_0 and interaction c . Crucial to the emergence of flat band in such systems, as is pointed out in Ref. [9], is the interplay between the SOC parameters (γ and Ω) and the lattice strength (V_0). The basic mechanism can be intuitively described using the single-particle picture [9]: (i) Without the interaction ($c = 0$) and the optical potential ($V_0 = 0$), the single-particle Hamiltonian H_0 can be cast into a dimensionless form

$$H_0 = \begin{pmatrix} \frac{k^2}{2} + \gamma k & \Omega \\ \Omega & \frac{k^2}{2} - \gamma k \end{pmatrix}, \quad (4)$$

which has two energy bands $\mu_{\pm}(k) = k^2/2 \pm \sqrt{\gamma^2 k^2 + \Omega^2}$ separated by a band gap 2Ω at $k = 0$. (ii) When an optical lattice ($V_0 \neq 0$) is added to Hamiltonian (4), a second band gap will open at the edge of Brillouin Zone, with the magnitude of the gap being dependent on V_0 . (iii) By engineering (via tuning γ , Ω and V_0) the magnitude of both gap, a flat band can be realized. Strikingly, the existence of flat bands stays robust against the mean-field interaction in the BEC according to Ref. [9].

In Figs. 2 (a1)-(d1), we have plotted the lowest Bloch bands $E_g(k)$ for various choices of the SOC parameters (γ and Ω) and lattice strength V_0 by numerically solving Eq. (1) with fixed interaction parameter c (detailed numerical method can be found in Ref. [24]). The presence of flat band is manifest to the eye (see Fig.2 (b1), (c1) and (d1)), as compared to an ordinary band (see Fig.2 (a1)). Quantitatively, the global flatness of the bands can be measured by the ratio W between the band gap and the band width [9].

Characterizing local flatness near the band minima.— When the model BEC system is probed by the Bragg spectroscopy, it is the excitation near the band minima k_{min} that is addressed in the linear perturbation regime. Therefore, we expect the *local flatness* at k_{min} to be directly probed in the Bragg spectroscopy, rather than the global flatness measured by W .

In order to characterize the local flatness near the band minima, we have calculated the effective mass $m^*(k_{\text{min}})$ for various bands (in this work, whenever we use the notation m^* , we refer to the effective mass evaluated at k_{min}). Our calculation shows that an ordinary band has $m^* \sim 1$ (e.g. $1/m^* = 0.65$ in Fig. 3 (a1)), while in comparison, the flat band has much larger effective mass $m^* \gg 1$ as expected (see Figs. 3 (b1)-(d1)). Interestingly, m^* also varies sharply for various flat band, such that we can further discriminate between the sectional flat band (see Figs. 2 (c1)-(d1)) and the global flat band (see Figs.2 (b1)), the former having much bigger effective mass m^* than the latter. In other words, the sectional band is *locally* much flatter near k_{min} than the global flat band, even though its global flatness measured by W can

be actually smaller. Figure 2 (b1) presents a typical globally flat band, which has $1/m^* = 0.059$; whereas, Figs.2 (c1) and (d1) present two sectional flat band, which have $1/m^* = 0.0038$ and $1/m^* = 0.00029$, respectively. Noticing that $m^* \rightarrow \infty$ for the sectional band in Fig. 2 (d1), we shall call it as a perfect flat band. As we shall see, the excitation behaviour of the model BEC can alter significantly when m^* and the flatness of band changes.

Probing flat bands using Bragg spectroscopy— We now discuss how the flatness of a band in a SO coupled BEC (see Fig. 1) can be revealed in the Bragg spectroscopy. The Bragg spectroscopy consists here in generating a density perturbation to the model system by using two laser beams that have momenta $\mathbf{k}_{1,2}$ and a frequency difference ω (ω is much smaller than their detuning from an atomic resonance [13, 14]). The linear perturbation is described by the Hamiltonian $V_1 = \frac{V}{2} [\rho_{\mathbf{q}}^\dagger e^{-i\omega t} + \rho_{-\mathbf{q}} e^{+i\omega t}]$, where $\rho_{\mathbf{q}} = \sum_j e^{i\mathbf{q}\cdot\mathbf{r}_j/\hbar}$ is the Fourier transformed one-body density operator, and $\mathbf{q} = \mathbf{k}_1 - \mathbf{k}_2$ is the probe momenta. Right after the perturbation, the dynamical structure factor [27, 28] is probed, which is written as

$$S(\mathbf{q}, \omega) = \sum_e |\langle e | \rho_{\mathbf{q}}^\dagger | 0 \rangle|^2 \delta(\omega - (E_e - E_g)/\hbar), \quad (5)$$

$$M = \begin{pmatrix} L^{(\uparrow\downarrow)}(k+q) & c\phi_{\uparrow 0}^2 & \Omega + c\phi_{\uparrow 0}\phi_{\downarrow 0}^* & c\phi_{\uparrow 0}\phi_{\downarrow 0} \\ -c(\phi_{\uparrow 0}^*)^2 & -L^{(\uparrow\downarrow)*}(k-q) & -c\phi_{\uparrow 0}^*\phi_{\downarrow 0}^* & -\Omega - c\phi_{\uparrow 0}^*\phi_{\downarrow 0} \\ \Omega + c\phi_{\uparrow 0}^*\phi_{\downarrow 0} & c\phi_{\downarrow 0}\phi_{\uparrow 0} & L^{(\downarrow\uparrow)*}(-k-q) & c\phi_{\downarrow 0}^2 \\ -c\phi_{\uparrow 0}^*\phi_{\downarrow 0}^* & -\Omega - c\phi_{\downarrow 0}^*\phi_{\uparrow 0} & -c(\phi_{\downarrow 0}^*)^2 & -L^{(\downarrow\uparrow)}(-k+q), \end{pmatrix} \quad (7)$$

with

$$L^{(m_1 m_2)}(k) = -\frac{1}{2}(2in + ik)^2 + V_0 \sin^2(x) - i\gamma(2in + ik) - \mu + 2c|\phi_{m_1 0}|^2 + c|\phi_{m_2 0}|^2, \quad (8)$$

and $m_1, m_2 = \uparrow, \downarrow$. By solving the BDG equations numerically, the Bogoliubov excitation spectrum can be straightforwardly extracted. Note that, in order to avoid the dynamic instability, we shall limit ourselves to the stable parameter regime [9]. Then the dynamic structure factor can be straightforwardly found via [29] $S(q, \omega) = \sum_j Z_j(q) \delta(\omega - \omega_j(q))$, where $Z_j(q)$ and $\omega_j(q)$ are the excitation strength and frequency from the ground state to the j -th Bloch band, respectively. In particular, the static structure factor for the model system can be immediately read off as

$$S(q) = \sum_j Z_j(q). \quad (9)$$

We present in Figs. (3) (a1)-(d1) the low-energy excitation spectrum of an optically trapped BEC with SOC corresponding to the four bands in Fig. 2, respectively. We find that, when the model BEC has an ordinary band, the familiar linear relation $\epsilon(q) \sim q$ arises (Fig. 3 (a1));

with $|0\rangle$ ($|e\rangle$) being the ground (excited) state having the energy E_g (E_e). From the dynamic structure factor, the excitation spectrum can then be extracted [28].

Let us calculate the excitation spectrum and the dynamic structure factor $S(q, \omega)$ of the model system for various band structures, from an ordinary band to a perfect flat band. For this purpose, we apply the Bogoliubov theory [29] to Eq. (1) and decompose the condensate wave function $(\psi_\uparrow, \psi_\downarrow)^T$ into the ground state wave function $(\phi_{\uparrow 0}, \phi_{\downarrow 0})^T$ and a small fluctuating term reading

$$\begin{pmatrix} \psi_\uparrow \\ \psi_\downarrow \end{pmatrix} = e^{-i\mu t} \left[\begin{pmatrix} \phi_{\uparrow 0} \\ \phi_{\downarrow 0} \end{pmatrix} + \begin{pmatrix} u_\uparrow(x) \\ u_\downarrow(x) \end{pmatrix} e^{-i\omega t} + \begin{pmatrix} v_\uparrow^*(x) \\ v_\downarrow^*(x) \end{pmatrix} e^{i\omega t} \right]. \quad (6)$$

By substituting Eq. (6) into Eq. (1) and expanding $u_{\uparrow, \downarrow}(x)$ and $v_{\uparrow, \downarrow}(x)$ in the Bloch form in terms of u_l and v_l (l labels the Bloch eigenstate), we obtain the Bogoliubov-de Gennes (BDG) equations $M\Delta\phi = \omega\Delta\phi$, with $\Delta\phi = (u_{\uparrow l}, v_{\uparrow l}, u_{\downarrow l}, v_{\downarrow l})$ and $\int dx (|u_{\uparrow l}|^2 - |v_{\uparrow l}|^2 + |u_{\downarrow l}|^2 - |v_{\downarrow l}|^2) = 1$, and the matrix M reads

whereas, remarkably, when the model BEC has a perfect flat band, a quadratic dispersion $\epsilon(q) \sim q^2$ emerges (Fig. 3 (d1)). Such distinct change in the excitation behaviour of the model system when the band flatness varies is also clearly observed in the dynamic structure, which are shown in Figs 3 (a2)- (d2). In particular, the static structure factor (see black solid lines in Figs. 3 (a2)-(d2)) exhibits a crossover from a linear relation $S(\mathbf{q}) \sim q$ to a quadratic relation $S(\mathbf{q}) \sim q^2$, when the band structure transforms from the ordinary into the perfect flat.

The crossover from the linear dispersion $\epsilon(q) \sim q$ to the quadratic dispersion $\epsilon(q) \sim q^2$ in the excitation spectrum of the model BEC, when the band structure transits from an ordinary band to a locally perfect flat, can be intuitively understood in connection with the effective mass m^* near the band minima. As previously mentioned, a perfect flat band is associated with an almost infinite effective mass $m^* \rightarrow \infty$, therefore, the q^2 term is expected to vanish in the single-particle dispersion relation $\epsilon_0(q)$

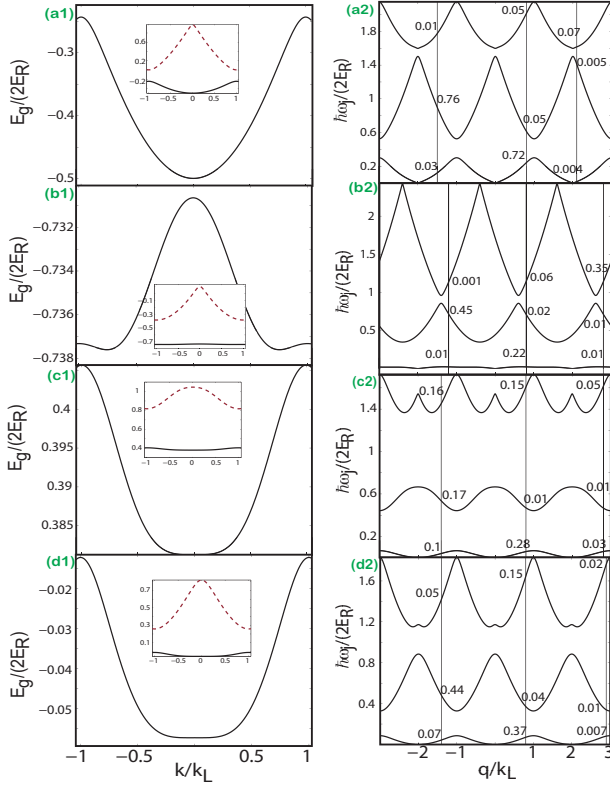


FIG. 2. (color online) (a1-d1) are the lowest Bloch band of an optically-trapped SO coupled BEC (in the insert, the lowest two Bloch bands are plotted); (a2-d2) are the lowest three Bogoliubov bands ω_j and the vertical lines represent the excitation strengths Z_j ($j = 1, 2, 3$) toward the first three bands for $q = 0.8k_L$, $q = -1.2k_L$, $q = 2.8k_L$ respectively. The parameters are given as follows: (a1, a2) $\gamma = 0.5000$, $V_0 = 0.6000$, and $\Omega = 0.8000$; (b1, b2) $\gamma = 1.0500$, $V_0 = 1.0000$, and $\Omega = 1.1500$; (c1, c2) $\gamma = 0.6100$, $V_0 = 2.0000$, and $\Omega = 0.3700$; (d1, d2) $\gamma = 0.7000$, $V_0 = 1.0000$, and $\Omega = 0.5005$.

(corresponding to zero kinetic energy) and the leading term can only emerge as $\epsilon_0(q) \sim q^4$. Thus, by using above results $S(q) \sim q^2$ for a perfect flat band and Feynman's relation $\epsilon(q) = \epsilon_0(q)/S(q)$, we immediately have $\epsilon(q) \sim q^2$ which explains the numerical results in Figs. 3 (c1) and (d1). In contrast, in the opposite case of an ordinary band when $m^* \sim 1$, the single-particle kinetic energy is finite such that $\epsilon_0(q) \sim q^2$. Hence from $S(q) \sim q$ and Feynman's relation, we have the familiar linear relation $\epsilon(q) \sim q$ in the BEC. We point out that, while the existence of flat bands in an optically trapped quasi-1D BEC with SOC can be described with a single-particle picture, the emerging quadratic low-energy dispersion when the band is perfectly flat is a many-body effect, which results from the interplay between the mean-field interaction, optical lattice, and SOC effect.

Finally, we have also analyzed how the excitation strength Z_j is affected by the lattice strength V_0 , in cases when the band is ordinary (Fig. 2(a1)) and when the band is flat (Figs. 2(b1)-(d1)), respectively. As is clearly

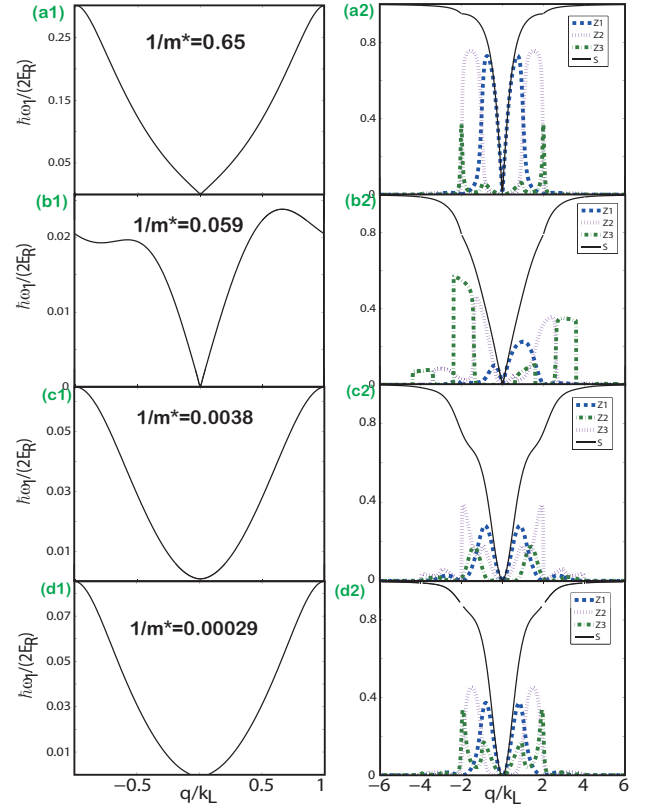


FIG. 3. (color online) (a1-d1) are the lowest excitation spectrum while (a2-d2) are the excitation strength ($Z_{1,2,3}$) and static structure factor (S) via a given transferred momentum q . Here, m^* labels the effective mass at the energy minima k_{min} . All the parameters here are the same as the corresponding ones in Fig. 2. For example, the parameters in Fig. 3 (b1) are same with ones in Fig. 2 (b1)

shown in Figs 2 (a2)-(d2), where the first three Bogoliubov bands are plotted, the dynamic structure factor is significantly affected by the optical lattice compared to the free-space case [22]. In particular, for a given value of momentum transfer p , it is possible to excite several states corresponding to different bands. For example, Fig. 2 (d2) shows that when a density perturbation with $q = 0.8k_L$ is generated in the BEC, not only the first excitation strength $Z_1 = 0.37$ is obtained, but also the second excitation $Z_2 = 0.04$. An important consequence is that, on one hand, it is possible to excite the high energy states with small values of p ; on the other hand, one can also excite the low energy states in the lowest band with high momenta p outside the first Brillouin zone. Such excitation behaviour is shared by both the ordinary band (Fig. 3 (b1)) and the flat bands (Figs. 3 (b2)-(d2)), and therefore, the existence of flat bands cannot be revealed in the excitation strength Z_j alone.

Overall, the crossover from linear to quadratic dispersion in the low-energy excitation spectrum presents a striking manifestation of the transition of an ordinary band into a perfect flat band, which permits the direct

probe of flat band using the Bragg Spectroscopy. The experimental realisation of our scenario amounts to controlling four parameters whose interplay underlies the physics of this work: the lattice strength V_0 , SOC parameters γ and Ω , and the interatomic interaction c . All these parameters are highly controllable in the state-of-the-art technologies: V_0 can be changed from $0E_R$ to $32E_R$ almost at will; both γ and Ω can be changed by varying the angle between the two Raman lasers or through a fast modulation of the laser intensities; in typical experiments to date, we can calculate the interaction coupling $c = 0.05$ with the relevant parameters [18] of $a = 100a_B$ with a_B the Bohr radius. Thus, we expect the phenomena discussed in this work be observable within the current experimental capability.

Conclusions and outlook.— To conclude, we have found that the excitation spectrum of an optically trapped quasi-1D BEC with SOC alters significantly when the band flatness varies. In particular, when the model BEC exhibits a perfect flat band (corresponding to $m^* \rightarrow \infty$ at the band minima), a quadratic dispersion $\epsilon(q) \sim q^2$ emerges in the low-energy part of the excitation spectrum; whereas, if the band is ordinary, the familiar

linear dispersion $\epsilon(q) \sim q$ arises. The variation in the flatness of band also alters the dynamic structure significantly, in particular, the static structure factor for a perfect band is quadratic in momenta $S(q) \sim q^2$, in contrast to the case of an ordinary band when $S(q) \sim q$ is linear. Based on these results, we propose to use Bragg spectroscopy to probe the arising flat band in an optically trapped quasi-1D BEC. The experimental verification of the new dynamic features predicted in this work is expected to provide a significant advance in our understanding of systems exhibiting flat band related phenomena.

Note added. After finishing our manuscript, we became aware of the work reported in Refs. [30–32], where the authors considered how to use Bragg spectroscopy to probe the quadratic excitation spectrum of a SO coupled BEC in the roton-maxon regime. Nevertheless, our system is very different from theirs.

Acknowledgments. We thank Biao Wu, Qizhong Zhu, Li Mao and P. Chatle for stimulating discussions. This work is supported by the NSF of China (Grant No. 11274315). Ying Hu also acknowledges support by the Austrian Science Fund (FWF) through SFB F40 FOQUS.

-
- [1] R. Roy and S. L. Sondhi, *Physics* **4**, 46 (2011); E. Tang, J. W. Mei, and X. G. Wen, *Phys. Rev. Lett.* **106**, 236802 (2011); T. Neupert, L. Santos, C. Chamon, and C. Mudry, *Phys. Rev. Lett.* **106**, 236804 (2011); K. Sun, Z. Gu, H. Katsura, and S. Das Sarma, *Phys. Rev. Lett.* **106**, 236803 (2011); N. Regnault and B. A. Bernevig, *Phys. Rev. X* **1**, 021014 (2011); D. Wang, Z. Liu, J. P. Cao, and H. Fan, *Phys. Rev. Lett.* **111**, 186804 (2013); A. G. Grushin, Á. Gómez-León, and T. Neupert, *Phys. Rev. Lett.* **112**, 156801 (2014).
- [2] N. Y. Yao, C. R. Laumann, A. V. Gorshkov, S. D. Bennett, E. Demler, P. Zoller, and M. D. Lukin, *Phys. Rev. Lett.* **109**, 266804 (2012).
- [3] Y. Z. You, Z. Chen, X. Q. Sun, and H. Zhai, *Phys. Rev. Lett.* **109**, 265302 (2012).
- [4] N. Goldman and J. Dalibard, *Phys. Rev. X* **4** 031027 (2014)
- [5] S. Choudhury and E. J. Mueller, *Phys. Rev. A* **90** 013621 (2014).
- [6] F. Lin, C. W. Zhang, and V.W. Scarola, *Phys. Rev. Lett.* **112**, 110404 (2014).
- [7] E. J. Bergholtz and Z. Liu, *Int. J. Mod. Phys. B* **27**, 1330017 (2013)
- [8] L. D. Landau and E. M. Lifshitz, *Quantum Mechanics: Nonrelativistic Theory* (Pergamon, Oxford, 1977).
- [9] Y. Zhang and C. Zhang, *Phys. Rev. A* **87**, 023611 (2013).
- [10] D. Pines and P. Nozières, *The theory of quantum liquids* (Benjamin, New York, 1966), Vol. I; P. Nozières and D. Pines, *The theory of Quantum Liquids* (Addison-Wesley, Reading, MA, 1990), Vol. II.
- [11] P. S. He, R. Liao, and W. M. Liu, *Phys. Rev. A* **86**, 043632 (2012).
- [12] The conclusion in Ref. [11] suggests that the Feynman relation for a 3D SO coupled BEC in free space is not satisfied any more. We point out that our model in this work is different with the one in Ref. [11] as follows: (i) different types of SO coupling are used; (ii) we consider an optically-trapped SO coupled BEC while Ref. [11] studies the case in free space; (iii) we limit ourselves in quasi-1D, whereas Ref. [11] focuses on 3D case. In our case, we have double-checked that Feynman relation is still valid: (i) without SO coupling, our numerical results can agree well with the main results in Ref. [29]; (ii) with SO coupling, our numerical code can recover all the figures in Ref. [9]. Moreover, the main results in Ref. [22] also imply that Feynman relation is still valid for an optically-trapped SO coupled BEC.
- [13] P. T. Ernst, S. Götze, J. S. Krauser, K. Pyka, D. S. Lühmann, D. Pfannkuche and K. Sengstock, *Nat. Phys.* **6**, 56 (2010).
- [14] X. Du, S. Wan, E. Yesilada, C. Ryu, D. J. Heinzen Z. X. Liang and B. Wu, *New. J. Phys.* **12**, 083025 (2010).
- [15] J. Dalibard, F. Gerbier, G. Juzeliunas, and P. Öhberg, *Rev. Mod. Phys.* **83**, 1523 (2011).
- [16] H. Zhai, *Int. J. Mod. Phys. B.* **26**, 1230001 (2012).
- [17] V. Galitski and I. B. Spielman, *Nature (London)*, **494**, 49 (2013).
- [18] Y. J. Lin, R. L. Compton, K. Jiménez-García, J. V. Porto, and I. B. Spielman, *Nature (London)* **462**, 628 (2009); Y. J. Lin, K. Jiménez-García, and I. B. Spielman, *Nature (London)* **471**, 83 (2011).
- [19] P. Wang, *et al.*, *Phys. Rev. Lett.* **109**, 095301 (2012); L. Cheuk, *et al.*, *Phys. Rev. Lett.* **109**, 095302 (2012).
- [20] C. Wang, C. Gao, C. M. Jian, and H. Zhai, *Phys. Rev. Lett.* **105**, 160403 (2010).
- [21] Y. Zhang, L. Mao, and C. Zhang, *Phys. Rev. Lett.* **108**,

- 035302 (2012).
- [22] Y. Li, L. P. Pitaevskii, and S. Stringari, Phys. Rev. Lett. **108**, 225301 (2012); Y. Li, G. I. Martone, L. P. Pitaevskii, and S. Stringari, Phys. Rev. Lett. **110**, 235302 (2013).
 - [23] Q. Zhu, C. Zhang, and B. Wu, Europhys. Lett. **100**, 50003 (2012).
 - [24] Z. X. Liang, X. Dong, Z. D. Zhang, and B. Wu, Phys. Rev. A **78** 023622 (2008).
 - [25] J. Keeling, Phys. Rev. Lett. **107**, 080402 (2011).
 - [26] As pointed out by Ref. [25], the existence of the quadratic spectrum of long wavelength modes is invoked in reexamine explanation of superfluidity.
 - [27] D. M. Stamper-Kurn, *et al.*, Phys. Rev. Lett. **83** 2876 (1999).
 - [28] F. Zambelli, L. Pitaevskii, D.M. Stamper-Kurn, and S. Stringari, Phys. Rev. A **61** 063608 (2000).
 - [29] C. Menotti, M. Krämer, L. Pitaevskii, and S. Stringari, Phys. Rev. A **67** 053609 (2003).
 - [30] S. C. Ji, L. Zhang, X. T. Xu, Z. Wu, Y. Deng, S. Chen, and J. W. Pan, arXiv:1408.1755v1.
 - [31] L.-C. Ha, L. W. Clark, C. V. Parker, B. M. Anderson, and C. Chin, arXiv:1407.7157v1.
 - [32] M. A. Khamsehchi, Y. Zhang, C. Hamner, T. Busch, and P. Engels, arXiv:1409.5387v1.